Supplementary Information

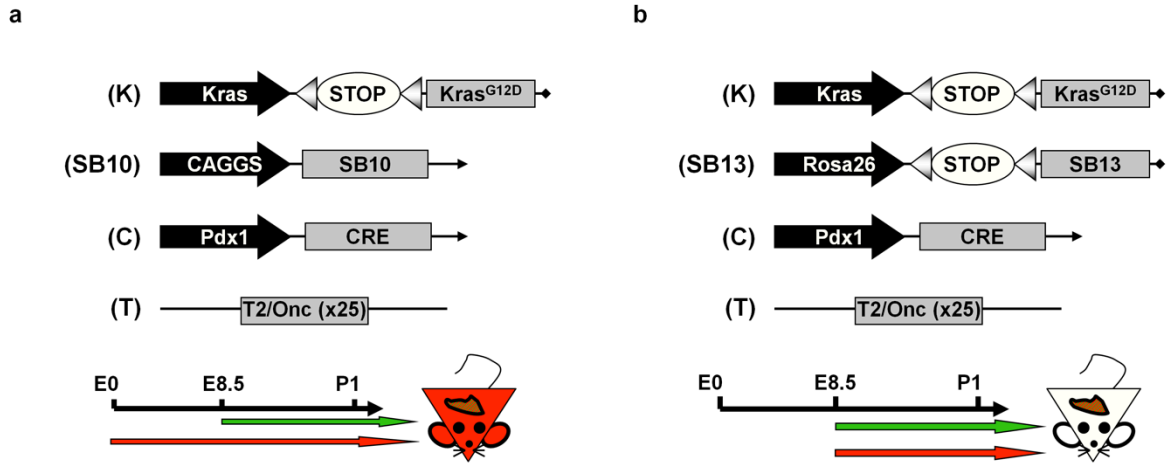

Supplementary Figure 1: Pérez-Mancera et al.

Supplementary Figure 1 | KCTSB10 and KCTSB13 cohorts. a, Scheme of the mutant alleles in the KCTSB10 (*Kras$^{LSL-G12D}$; Pdx1-cre; T2/Onc; CAGGS-SB10*) cohort. This cohort expresses *Kras^{G12D}* after E8.5 in pancreatic cell progenitors (green arrow) and *SB10* transposase in the whole soma as denoted by the color red. **b**, Scheme of the mutant alleles in the KCTSB13 (*Kras$^{LSL-G12D}$; Pdx1-cre; T2/Onc; Rosa26-LSL-SB13*) cohort. This cohort expresses both *Kras^{G12D}* and *SB13* transposase after E8.5 selectively in pancreatic cell progenitors. Triangles represent LoxP sites flanking the transcriptional STOP cassette.

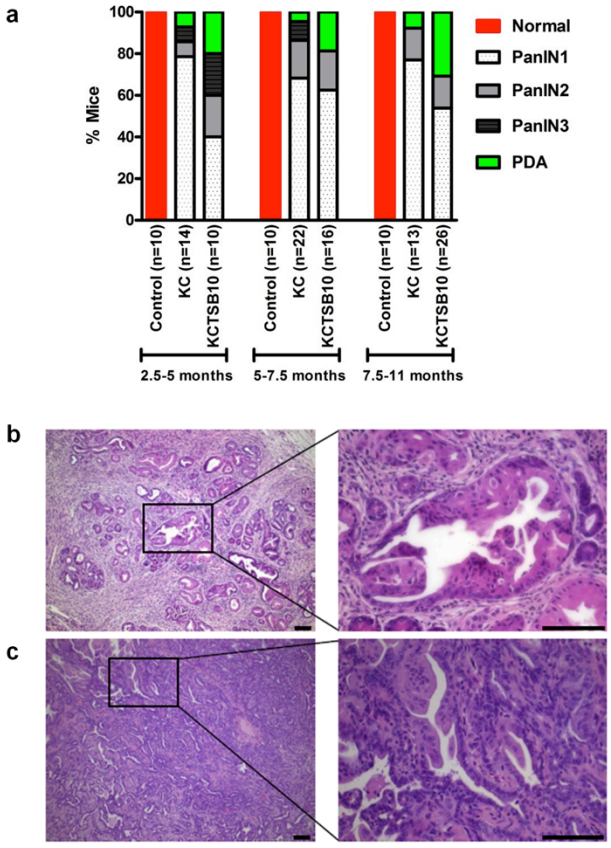

d

Cause of death	%
mPDA	24
NSCLC	24
Papilloma	15.5
Squamous Cell Carcinoma	7
Hepatocellular Carcinoma	3.5
Lymphoma/Thymoma	3.5
Found Dead	15.5
Other	7

Supplementary Figure 2: Pérez-Mancera et al.

Supplementary Figure 2 | SB10 transposon-mediated insertional mutagenesis accelerates the progression of ductal pancreatic cancer in mice. a-c, Constitutive and widespread SB10;T2/Onc transposition cooperates with $Kras^{G12D}$ to promote advanced mPanIN and mPDA. **a,** mPanIN to mPDA progression in *$Kras^{LSL-G12D}$; Pdx1-cre; T2/Onc; CAGGS-SB10* (KCTSB10) mice is increased compared to the KC cohort (*$Kras^{LSL-G12D}$; Pdx1-cre; T2/Onc* (KCT), *$Kras^{LSL-G12D}$; Pdx1-cre; CAGGS-SB10* (KCSB10) and *$Kras^{LSL-G12D}$; Pdx1-cre* (KC) mice) and the control cohort (*$Kras^{LSL-G12D}$; T2/Onc; CAGGS-SB10* (KTSB10) and *Pdx1-cre; T2/Onc; CAGGS-SB10* (CTSB10) mice). **b-c,** Representative histological sections of mPanIN3 (**b**) and mPDA (**c**) in KCTSB10 mice. Scale bar: 100µm. **d,** Phenotypes developed by the KCTSB10 mice. "mPDA": mouse Pancreatic Ductal Adenocarcinoma. "NSCLC": Non Small Cell Lung Carcinoma.

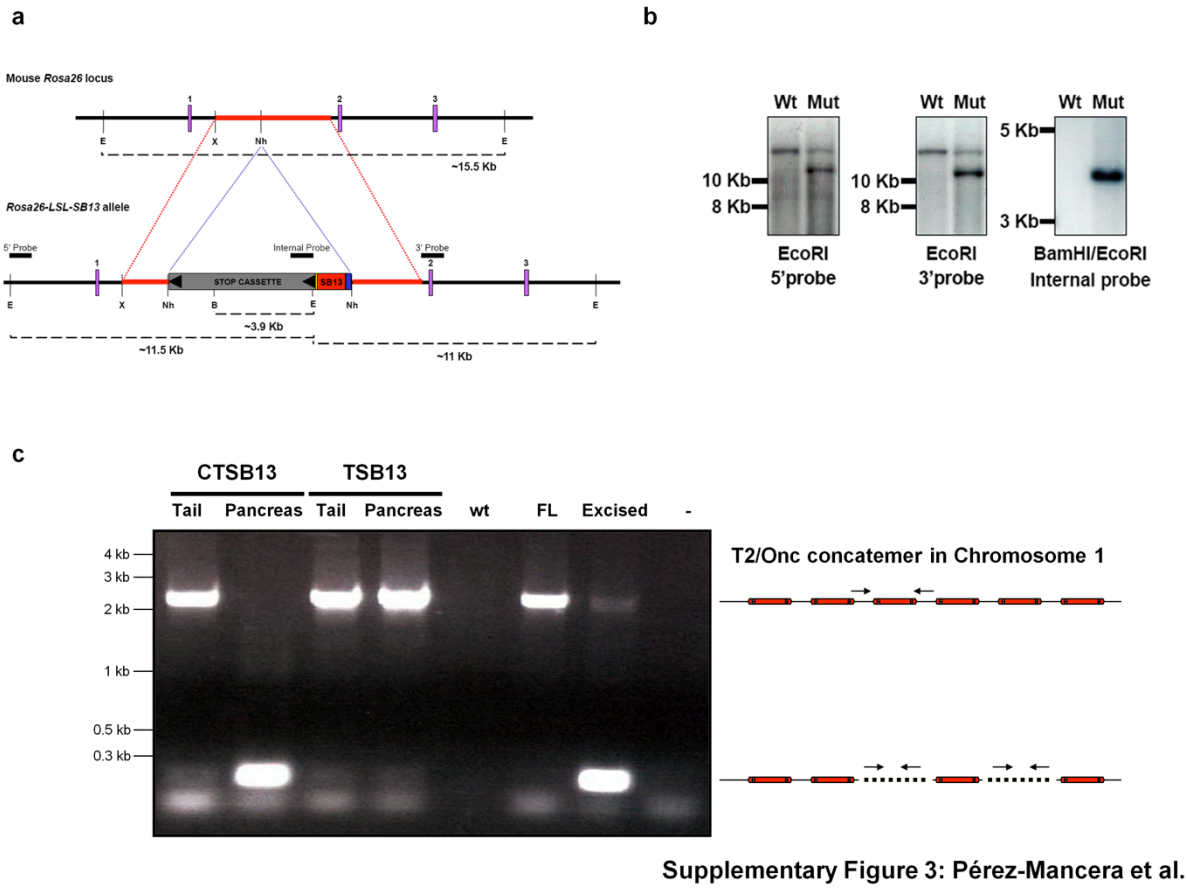

Supplementary Figure 3: Pérez-Mancera et al.

Supplementary Figure 3 | Generation of the *Rosa26-LSL-SB13* allele. a, The targeting construct pRosa26-LSL-SA-SB13-BGHpolyA, which harbours the hyperactive SB13 transposase[39], was inserted into the Rosa26 intronic sequence between exons 1 and 2. Rosa26 genomic DNA used in the targeting vector flanking DNA is shown in red; black triangles represent loxP sites flanking the transcriptional STOP cassette cloned upstream the SB13 cDNA; the yellow bar represents the splice acceptor sequence; and the blue rectangle represents the BGH polyadenylation sequence. (B: BamHI; E: EcoRI; Nh: NheI; X: XbaI). **b**, Southern blots of gDNA isolated from wild-type (WT) and targeted Rosa26-LSL-SB13 (Mut) TL1 ES cell clones confirming the correct integration of the pRosa26-LSL-SA-SB13-BGHpolyA targeting vector. Probe locations and expected DNA fragment mobilities are shown in (**a**). **c**, Confirmation of conditional activation of SB13 in pancreas but not tail tissue obtained from *Pdx1-cre; T2/Onc; Rosa26-LSL-SB13* (CTSB13) mice. In the intact T2/Onc concatemer the band has a migration of ~2.2 Kb, whereas it has a migration of ~220 bp after transposition. In *T2/Onc; Rosa26-LSL-SB13* (TSB13) mice, the transposon concatemer remains intact. (wt: gDNA from control mouse. FL: gDNA from *T2/Onc* mouse with intact donor concatemer. Excised: gDNA from *T2/Onc;CAGGS-SB10* mouse. "-" denotes no gDNA added).

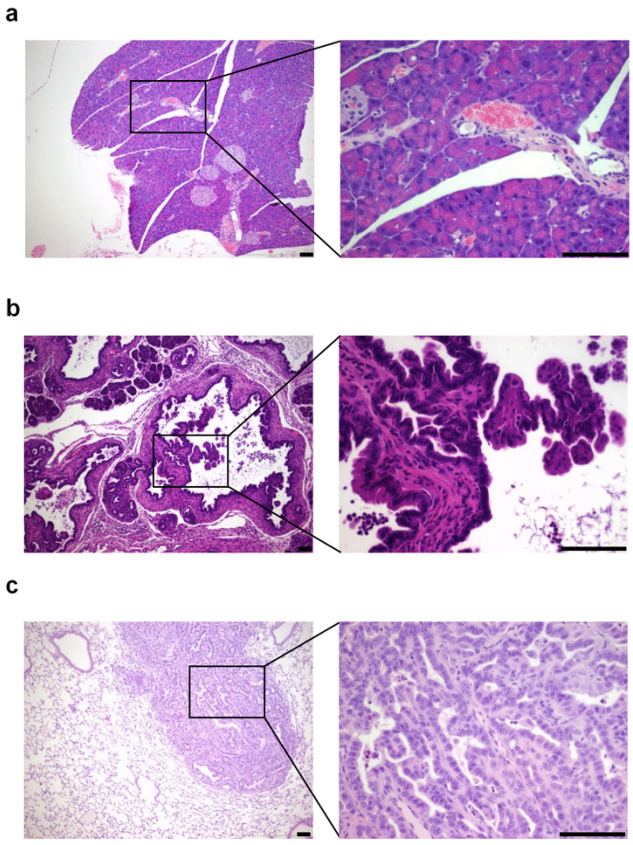

Supplementary Figure 4: Pérez-Mancera et al.

Supplementary Figure 4 | SB13;T2/Onc cooperates with *Kras*^{G12D} to promote the progression of PDA. a-c, Histological findings in pancreata and tumors from control and KCTSB13 mice. **a**, Representative histological section showing normal pancreas in CTSB13 mice. **b**, Histological section showing low-grade cystic papillary neoplasm observed in KCTSB13 mice. **c,** mPDA lung metastasis in KCTSB13 mice. Scale bar: 100 µm.

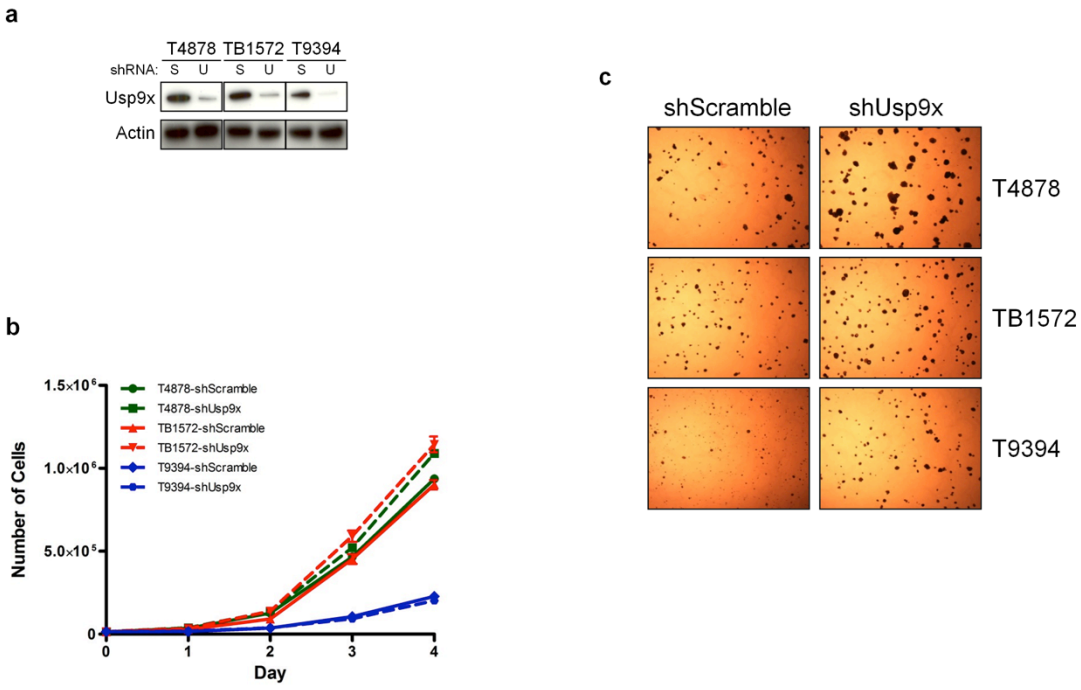

Supplementary Figure 5: Pérez-Mancera et al.

Supplementary Figure 5 | Usp9x knock-down does not increase cell proliferation in monolayer cultures. **a**, shRNA efficiently knocks down Usp9x in 3 different mouse PDA cell lines. Actin is used as loading control. (S: Scramble. U: Usp9x). **b**, Usp9x knockdown has no effect on cell proliferation in 2-dimensional monolayers. The mean and s.e.m. of a representative experiment performed in triplicate are shown. **c**, Usp9x knockdown promotes anchorage-independent growth of mouse KC tumor cell lines in soft agar.

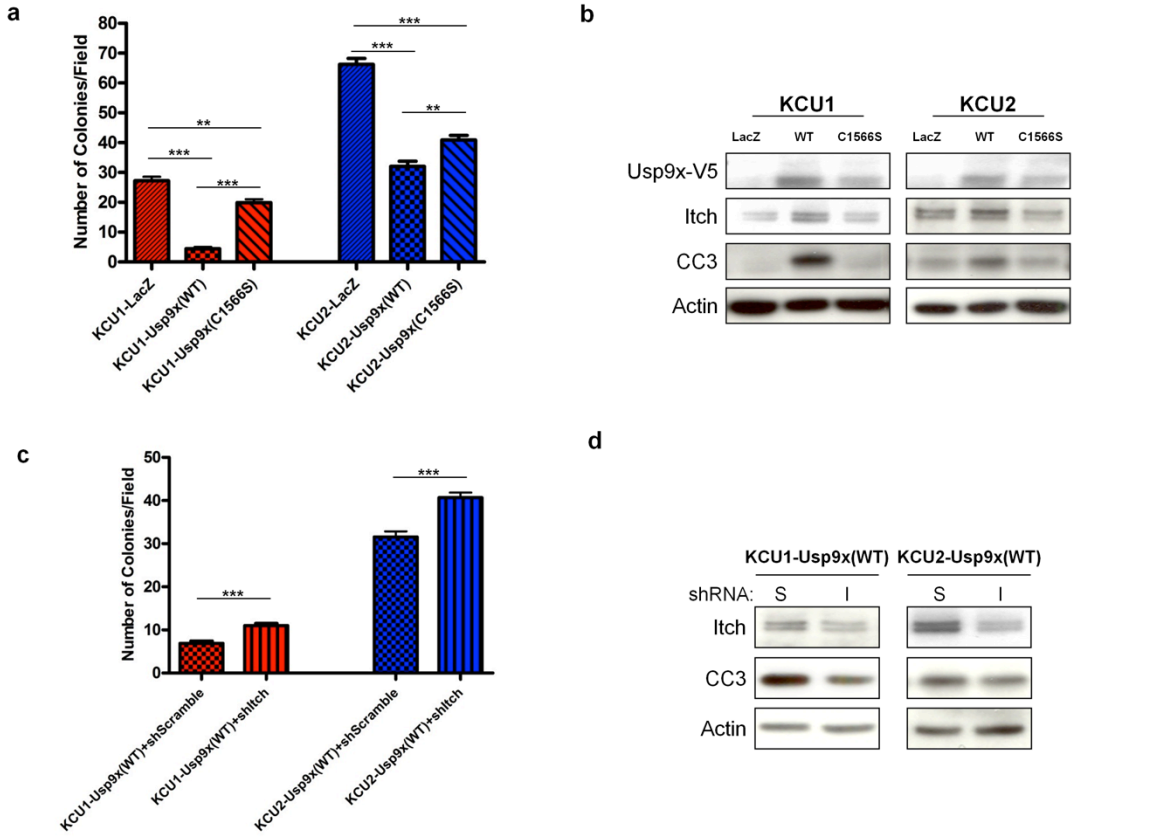

Supplementary Figure 6: Pérez-Mancera et al.

Supplementary Figure 6 | Usp9x expression reverts transformation *in vitro* in Usp9x null cell lines. **a,** Ectopic Usp9x (WT) reduces anchorage-independent growth in soft agar of 2 mouse PDA tumor cell lines from KCU mice (KCU1 and KCU2), while the enzymatically inactive Usp9x (C1566S) isoform shows a modest effect. The mean and s.e.m. of one representative experiment performed in triplicate are shown (***, p<0.001; **, p<0.01; Mann Whitney test). **b**, Expression of Usp9x (WT), but not Usp9x (C1566S), induces Itch and anoikis in KCU1 and KCU2 tumor cell lines. Protein levels of Usp9x and cleaved caspase 3 (CC3) are shown following 4 days in suspension, with Actin loading control. **c-d**, The incomplete knock-down of Itch partially rescues anchorage-independent growth (**c**) and anoikis (**d**) in KCU1 and KCU2 cells ectopically expressing Usp9x (WT). The mean and s.e.m. of one representative experiment performed in triplicate are shown (***, p<0.001). (S: Scramble; I: Itch).

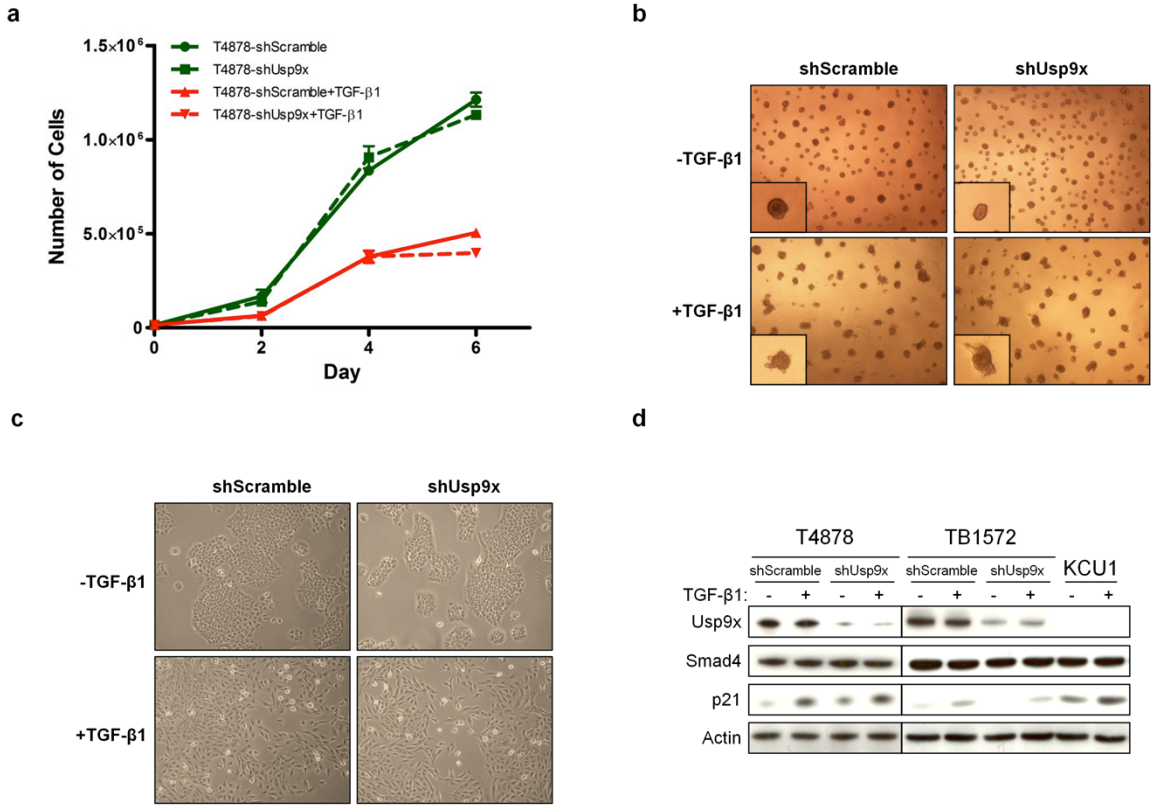

Supplementary Figure 7: Pérez-Mancera et al.

Supplementary Figure 7 | Usp9x loss does not impact SMAD4 or TGFβ function in pancreatic ductal cells. a, Mouse PDA cell line T4878 remains sensitive to TGF-β1 growth inhibition after Usp9x knockdown. The mean and s.e.m. of one representative experiment performed in triplicate are shown. **b,** Mouse PDA cell line T4878 undergoes TGF-β1-mediated morphological transformation in matrigel independent of Usp9x levels. **c**, TGF-β1 induces EMT of the cell line T4878 after TGF-β1 exposure despite downregulation of Usp9x. **d,** p21 protein levels are increased following TGF-β1 exposure irrespective of Usp9x expression in T4878, TB1572 and KCU1 cell lines.

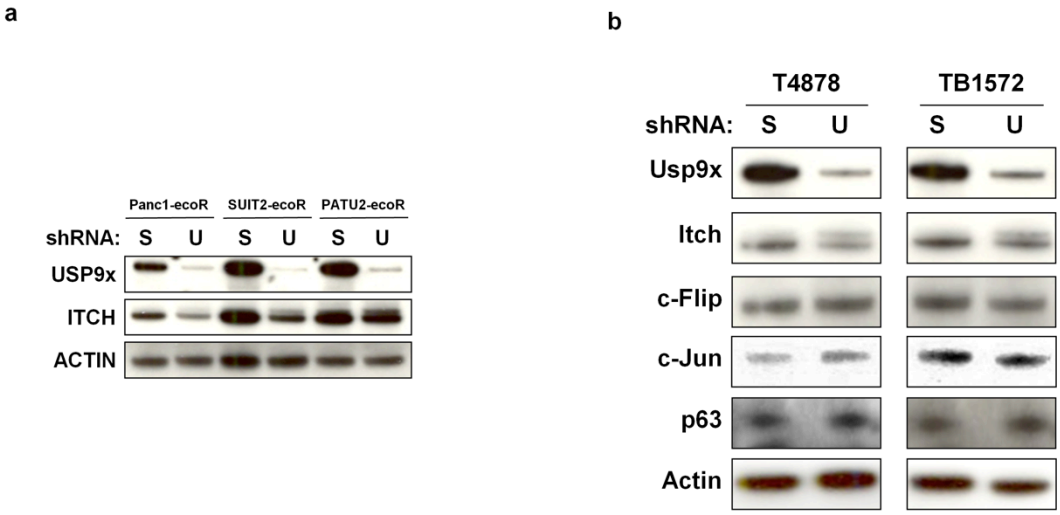

Supplementary Figure 8: Pérez-Mancera et al.

Supplementary Figure 8 | Usp9x controls Itch levels. a, USP9x knock-down induces ITCH down-regulation in the human PDA cell lines Panc1-ecoR, SUIT2-ecoR and PATU2-ecoR following 4 days in suspension, with Actin loading control. The anti-Itch immunoreactive band that migrates more slowly is consistent with the mobility of mono-ubiquitinated Itch. (S: Scramble; U: Usp9x). **b,** Usp9x knock-down in the T4878 and TB1572 cell lines does not markedly change the levels of expression of Itch substrates known to be associated with cell survival following 4 days in suspension. Actin is used as loading control. (S: Scramble; U: Usp9x).

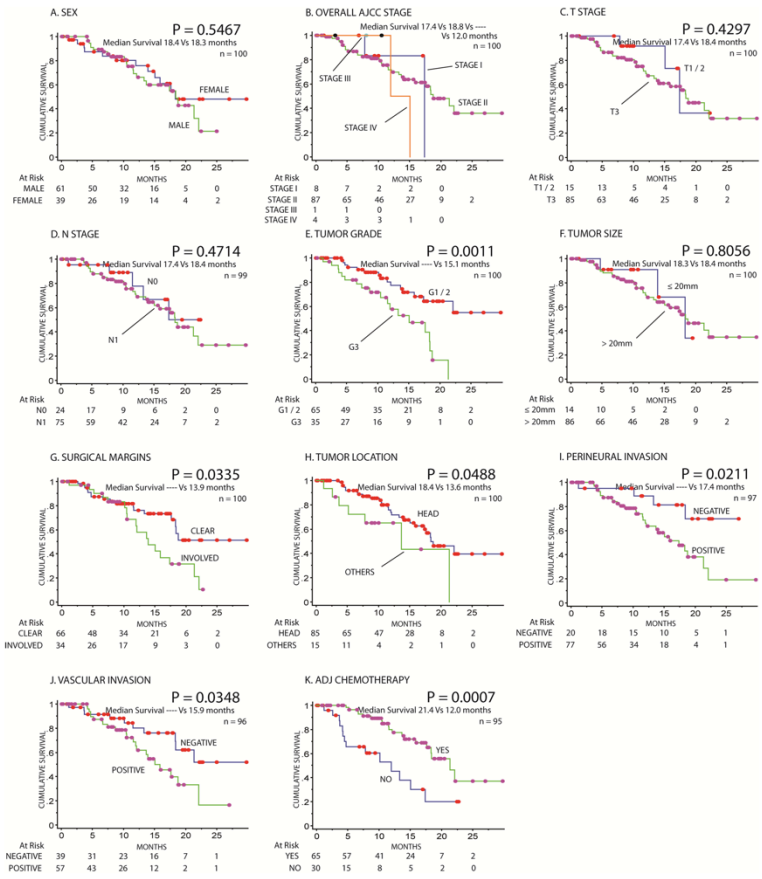

Supplementary Figure 9: Pérez-Mancera et al.

Supplementary Figure 9 | Clinical and Pathological parameters correlate with outcome in resected PDA from Australian cohort. By univariate analysis, tumor grade, perineural invasion, surgical margins, tumor location, vascular invasion, and adjuvant chemotherapy are all individual parameters that correlate with post-surgical survival. (----: Median survival has not been reached yet).

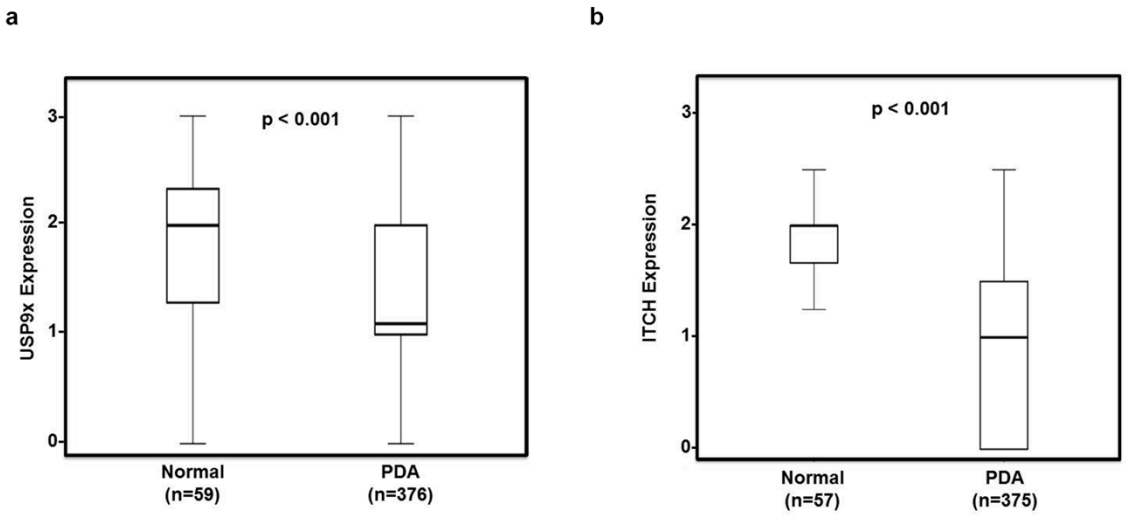

Supplementary Figure 10: Pérez-Mancera et al.

Supplementary Figure 10 | USP9X and ITCH expression are decreased in human PDA. a, Boxplot comparing USP9X protein expression by immunohistochemical detection in tissue samples from patients with PDA (n=376; median=1.1) and adjacent normal tissue (n=59; median=2) ($p<0.001$; Mann U test). **b**, Boxplot comparing ITCH protein expression by immunohistochemical detection in tissue samples from patients with PDA (n=375; median=1) and adjacent normal tissue (n=57; median=2) ($p<0.001$; Mann U test).

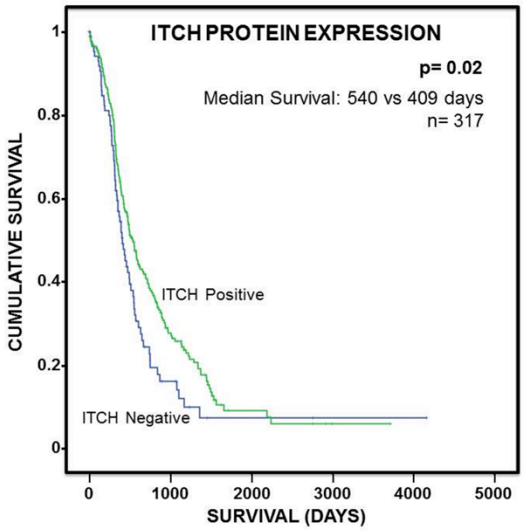

Supplementary Figure 11: Pérez-Mancera et al.

Supplementary Figure 11 | Low ITCH expression in human PDA correlates with poor clinical outcome. Kaplan-Meier survival curve comparing survival of individuals with resected PDA (n=317) and that either express (green, n=228) or lack (blue, n=89) expression of ITCH protein (median survival: 540 vs. 409 days, p=0.02; log-rank test).

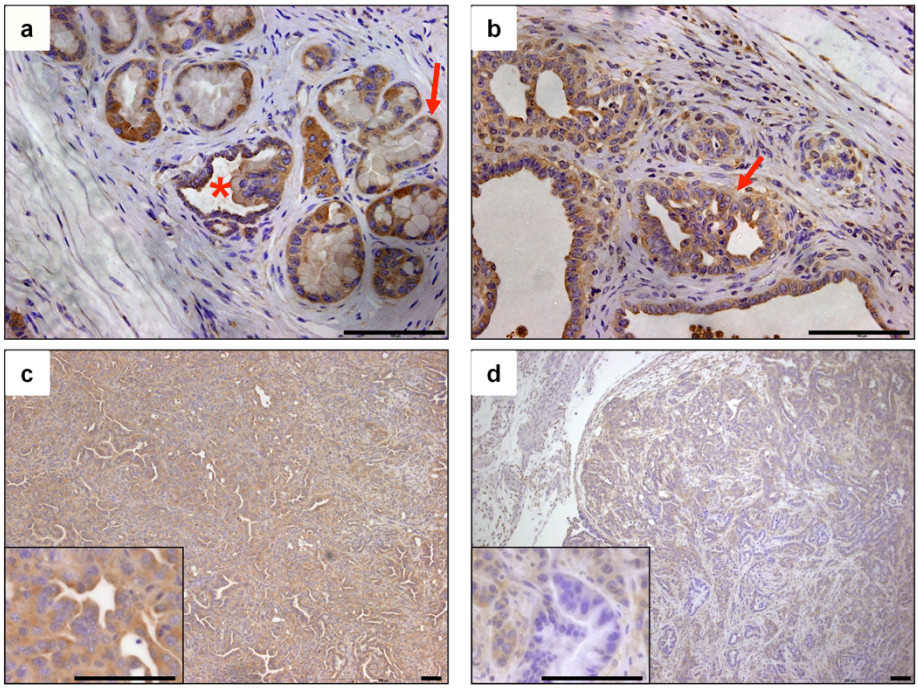

Supplementary Figure 12: Pérez-Mancera et al.

Supplementary Figure 12 | Usp9x is expressed in murine PanIN and lost focally in mPDA. a, Immunohistochemical analysis demonstrates that Usp9x is expressed in mPanIN1 (arrow) and mPanIN2 (asterisk) in *Kras*$^{LSL\text{-}G12D}$*; Pdx1-cre* mice (>10/10 each preneoplasm). **b,** mPanIN3 (arrow) uniformly express Usp9x (5/5 examined). **c-d,** Invasive mPDA tumors obtained from *Kras*$^{LSL\text{-}G12D}$*; Pdx1-cre* mice show a heterogeneous USP9x expression, with most tumors showing strong uniform expression (**c**), and others the focal absence of expression (**d**). Scale bar: 100 µm.

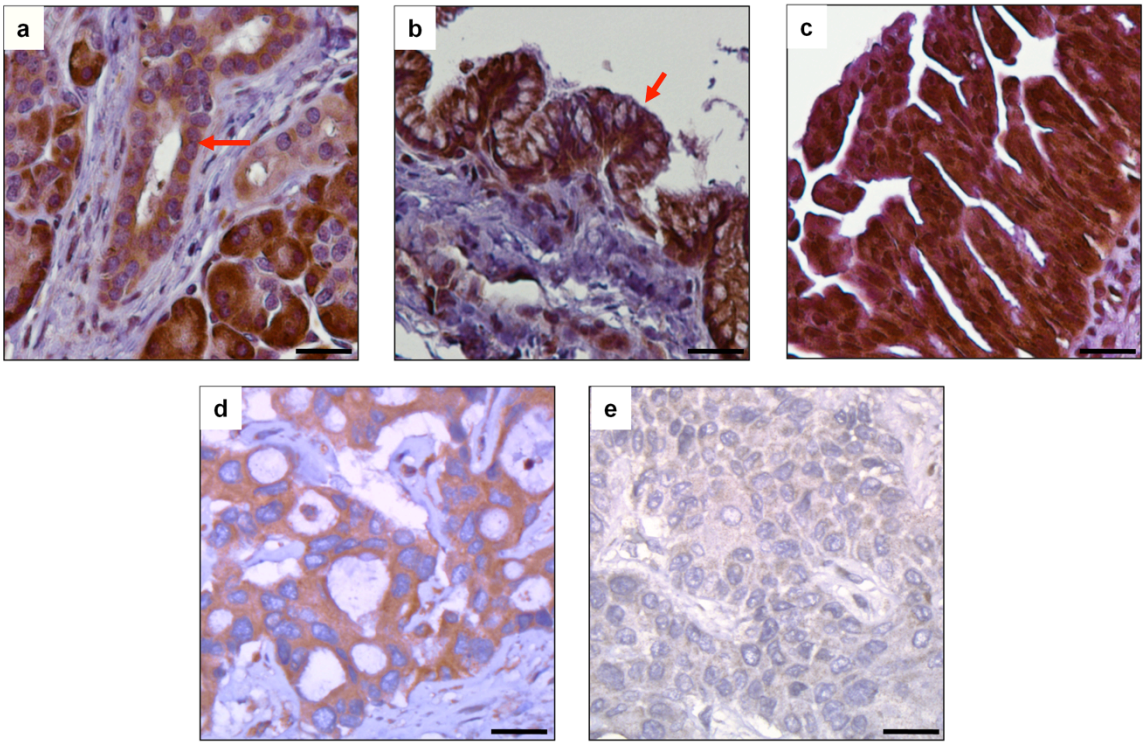

Supplementary Figure 13: Pérez-Mancera et al.

Supplementary Figure 13 | USP9X is expressed in human PanIN and lost in PDA. a-c, Immunohistochemical analysis demonstrates that USP9X is highly expressed in both normal pancreatic ductal cells (arrow) (**a**), and in 27/27 cases of human PanIN, with a representative PanIN1 (**b,** arrow), and PanIN3 (**c**). **d-e,** PDAs that either express (**d**), or lack (**e**) expression of USP9X. Scale bar: 200 µm.

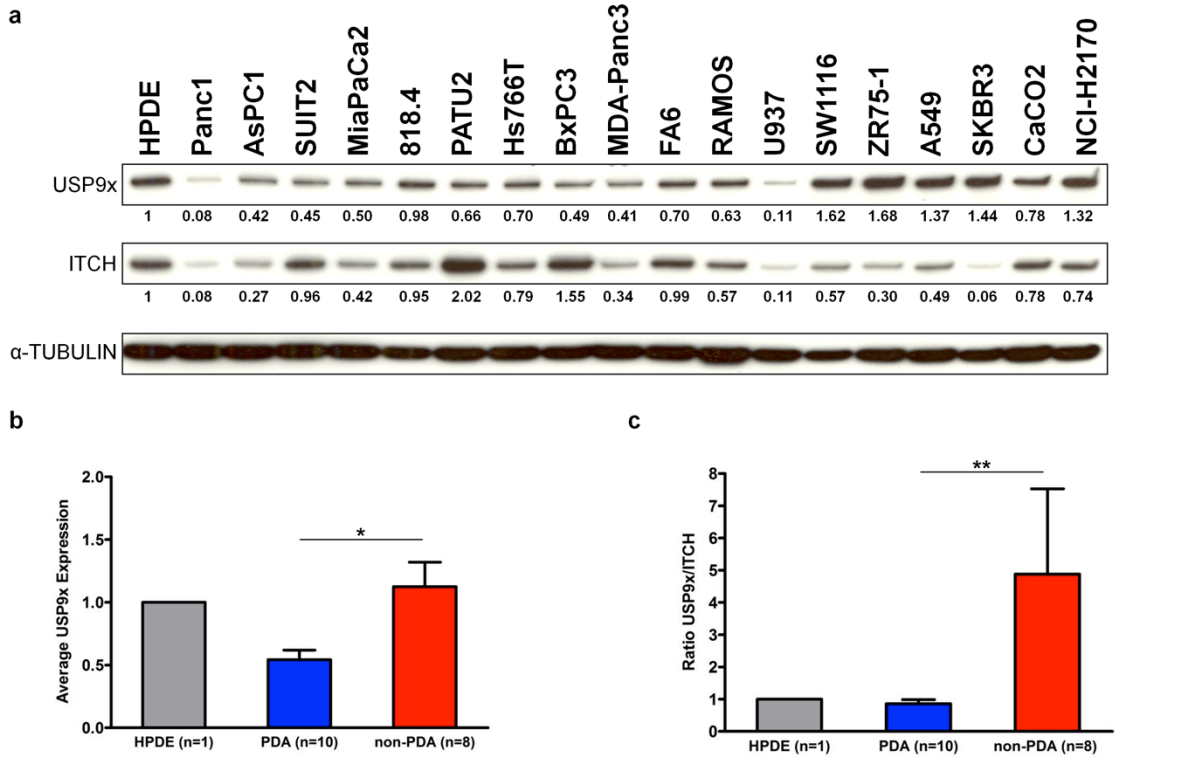

Supplementary Figure 14: Pérez-Mancera et al.

Supplementary Figure 14 |USP9X expression is lower in PDA than in other human cancer cell lines. **a,** Western-blot showing levels of expression of USP9X and ITCH in a panel of 10 PDA cell lines (AsPC1, BxPC3, Panc1, MiaPaCa2, 818.4, Hs766T, PATU2, SUIT2, FA6 and MDA-Panc3). The human pancreatic ductal cell line HPDE is used as comparison. The USP9X expression is also assessed in 2 colorectal cancer (CaCO2 and SW1116), 2 breast cancer (SKBR3 and ZR75-1), 2 lung cancer (A549 and NCI-H2170), 1 histiocytic lymphoma (U937) and 1 Burkitt's lymphoma (RAMOS) cell lines. α-TUBULIN is used as loading control. Relative expression was quantified with Image Quant TL software (GE Healthcare). **b,** Average expression of USP9X in HPDE (n=1), PDA (n=10) and non-PDA (n=8) tumor cell lines. The mean and s.e.m. are shown (*, $p<0.05$; Mann Whitney test). **c**, The ratio of USP9X/ITCH is characteristic of PDA cells in comparison to non-PDA cancer cell lines. The mean and s.e.m. are shown (**, $p<0.01$; Mann Whitney test).

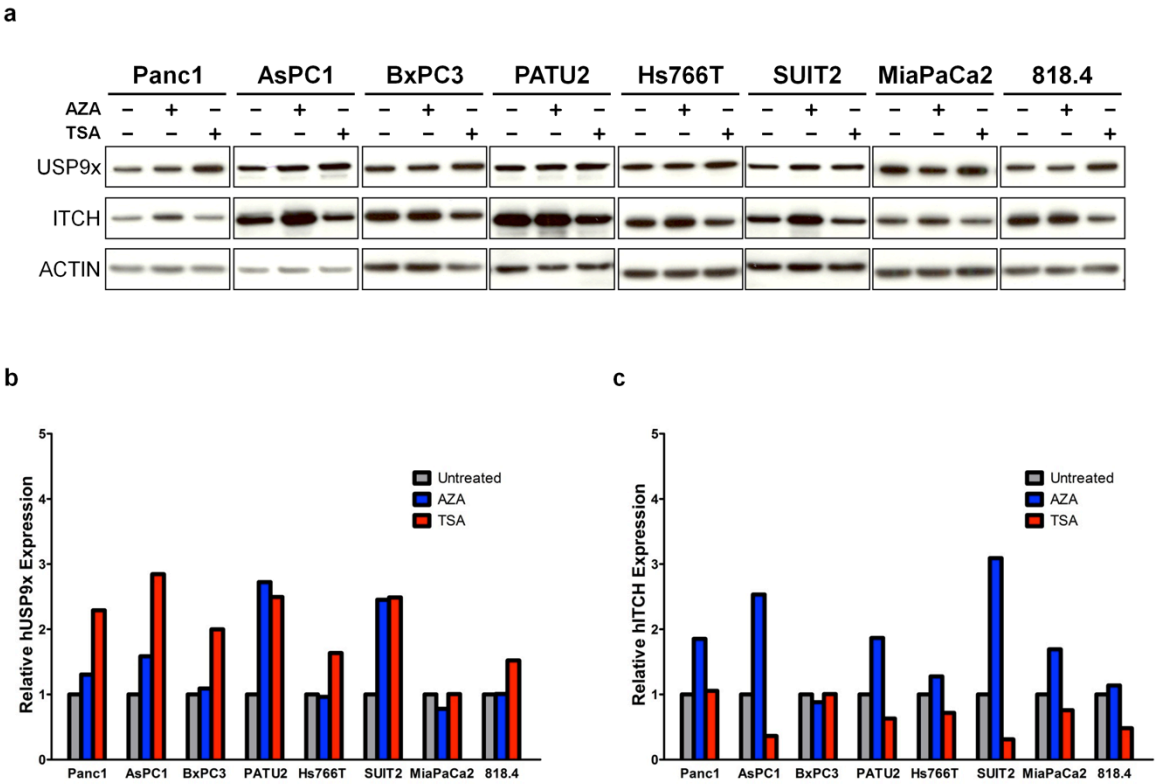

Supplementary Figure 15: Pérez-Mancera et al.

Supplementary Figure 15 | Trichostatin A and 5-Aza-2-deoxycytidine regulate USP9X and ITCH expression. a, Western blot analysis showing that trichostatin A (TSA) and 5-Aza-2-deoxycytidine (AZA) treatment modestly increases USP9X protein levels in some human PDA cell lines. ITCH protein levels are increased by AZA but not TSA. ACTIN is used as loading control. **b,** Densitometric quantification of USP9X protein levels. **c**, Densitometric quantification of ITCH protein levels. Relative expression was quantified with Image Quant TL software (GE Healthcare).

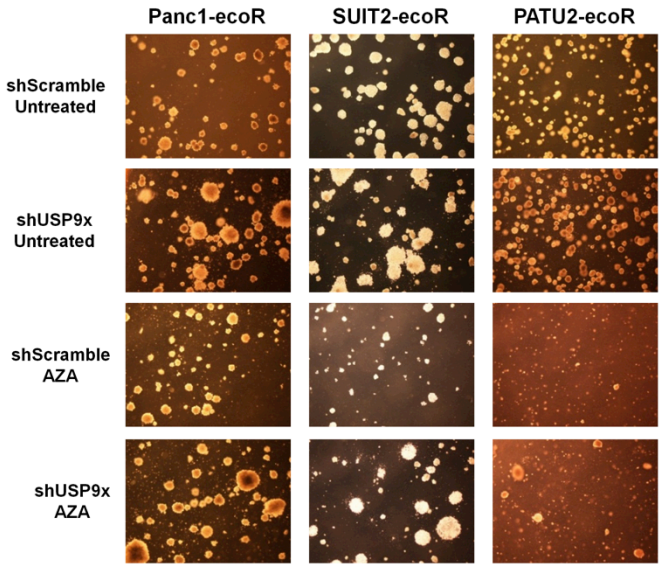

Supplementary Figure 16: Pérez-Mancera et al.

Supplementary Figure 16 | 5-Aza-2-deoxycytidine induced PDA cell death is partially rescued by USP9X ablation. USP9X knock-down in Panc1-ecoR, SUIT2-ecoR and PATU2-ecoR induces anchorage-independent growth in soft agar, and rescues colony formation that is suppressed by 5-Aza-2-deoxycytidine (AZA).

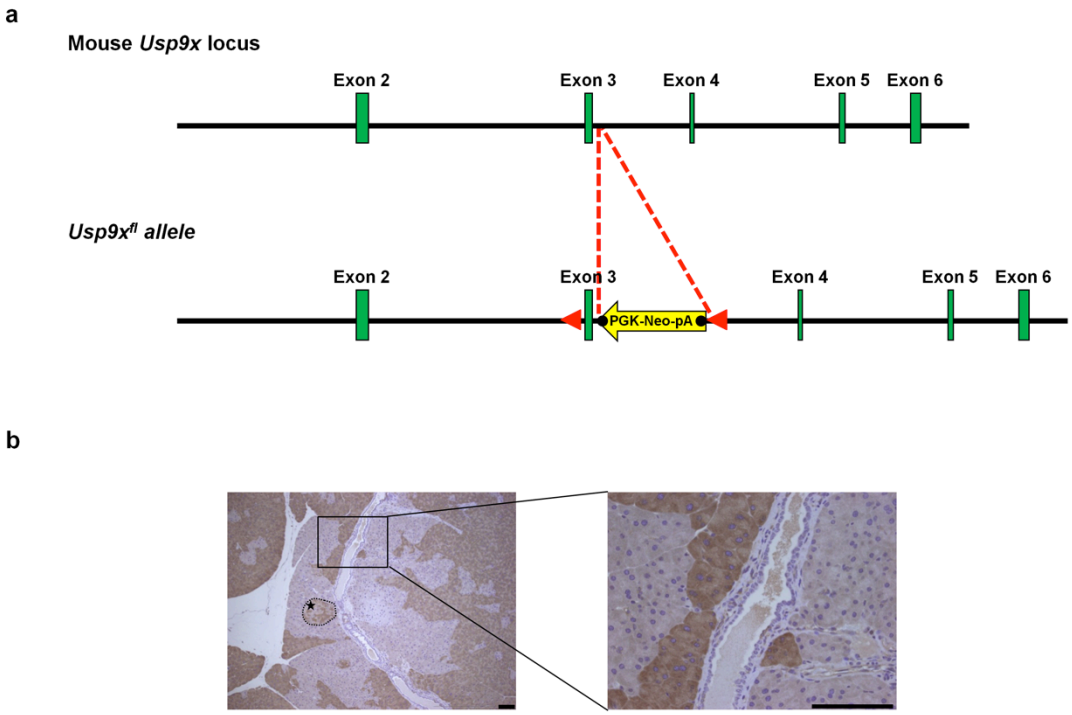

Supplementary Figure 17: Pérez-Mancera et al.

Supplementary Figure 17 | Generation of a conditional *Usp9x*^{fl} allele. a, *Usp9x*^{fl} targeting construct. Red triangles represent loxP sites flanking exon 3 of the endogenous *Usp9x* locus on chromosome X. Black circles in the PGK-Neo-pA cassette represent frt sites. **b,** Immunohistochemichal analysis showing the mosaic expression of Usp9x in pancreas from *Pdx1-cre; Usp9x*$^{fl/y}$ mice. This mosaic expression is observed in all pancreatic epithelial tissues, consistent with the known expression pattern on the Pdx1-cre transgene. The star represents an islet. Scale bar: 100 µm.

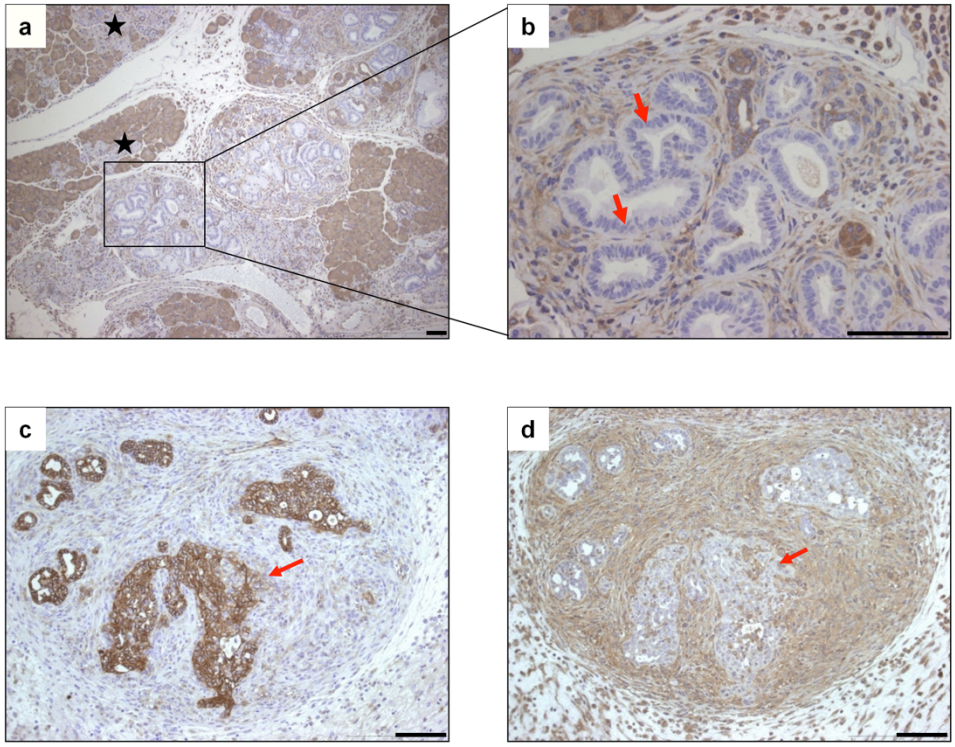

Supplementary Figure 18: Pérez-Mancera et al.

Supplementary Figure 18 | *Usp9x* loss accelerates tumorigenesis in vivo. a-b, Loss of *Usp9x* expression in heterozygous females**.** Immunohistochemical analysis demonstrates the loss of Usp9x expression in preneoplastic cells (arrows) in *Kras*$^{LSL\text{-}G12D}$*; Pdx1-cre; Usp9x*$^{fl/+}$ pancreas. The stroma and acinar compartment reveal intact Usp9x expression. Stars denote negative Usp9x reactivity in normal acinar tissue confirming the mosaic expression of the *Pdx1-cre* allele in the heterozygous female mice. Scale bar: 100 µm. **c-d,** *Usp9x* loss cooperates with *Kras*^{G12D} in pancreas to promote pancreatic carcinoma. E-cadherin is expressed (**c**) and Usp9x is absent (**d**) in a locally invasive pancreatic carcinoma (arrow) in 3 month old *Kras*$^{LSL\text{-}G12D}$*; Pdx1-cre; Usp9x*$^{fl/+}$ and *Kras*$^{LSL\text{-}G12D}$*; Pdx1-cre; Usp9x*$^{fl/y}$ mice. Scale bar: 100 µm.

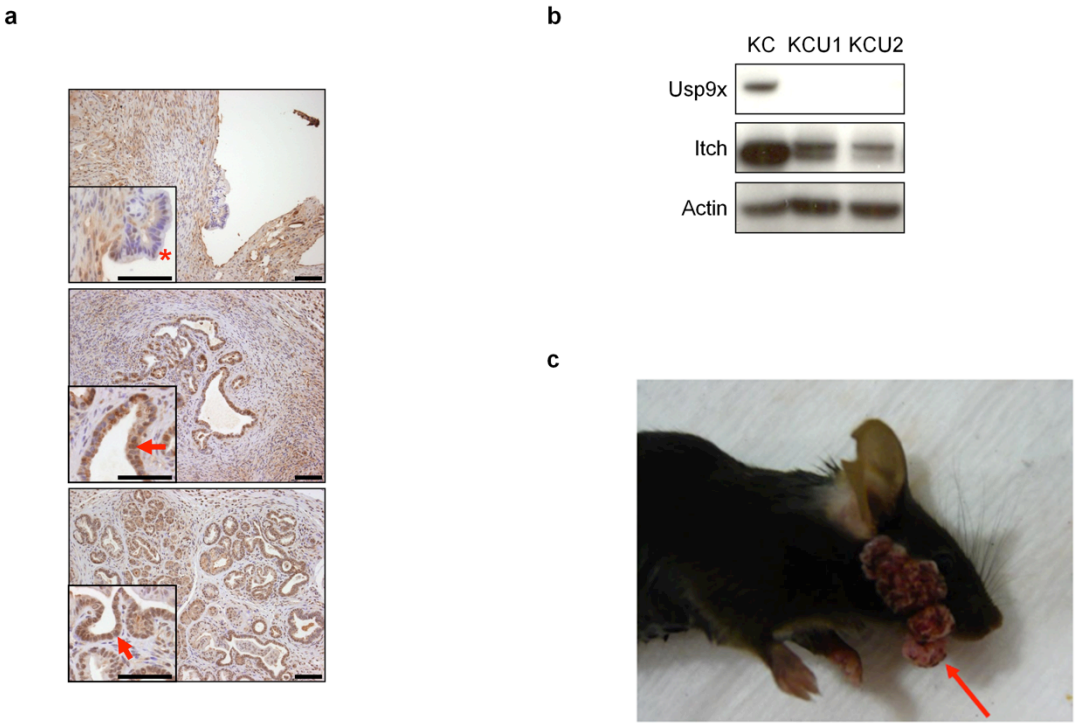

Supplementary Figure 19: Pérez-Mancera et al.

Supplementary Figure 19 | *Usp9x* loss influences the E3 ligase Itch and cooperates with *Kras*^{G12D} to promote papillomas. a, Immunohistochemical analysis demonstrates that the loss of Usp9x does not affect Smad4 nuclear localization (arrow) in KC (*Kras*$^{LSL\text{-}G12D}$*; Pdx1-cre)* (middle panel) and in KCU (*Kras*$^{LSL\text{-}G12D}$*; Pdx1-cre; Usp9x*$^{fl/y}$) (lower panel) mPanINs. The upper panel denotes negative Smad4 reactivity in a Smad4 null pancreatic neoplasm and included as a negative control (star). Scale bar: 100 µm. **b**, Western blot analysis of 2 early mouse cell lines established from *Kras*$^{LSL\text{-}G12D}$*; Pdx1-cre; Usp9x*$^{fl/+}$ and *Kras*$^{LSL\text{-}G12D}$*; Pdx1-cre; Usp9x*$^{fl/y}$ mice (KCU1 and KCU2) shows the absence of Usp9x and alterations in Itch mobility compared to a cell line expressing wild-type *Usp9x* (KC). **c,** *Kras*$^{LSL\text{-}G12D}$*; Pdx1-cre; Usp9x*$^{fl/y}$ and *Kras*$^{LSL\text{-}G12D}$*; Pdx1-cre; Usp9x*$^{fl/+}$ mice develop advanced skin papillomas (arrow) in the face and urogenital area at the age of 3 months.

Supplementary Table 1 | Candidate CISs in pancreas tumors from KCTSB10 mice.

Gene	Chr	CIS Peak Location	CIS Height	N	I	CIS Method	GKC Scale
Zc3h7b	15	81620444	3.9974	4	4	GKC	15000
Usp9x	X	12693219	4.0695	4	6	GKC	15000
CIS4:89197070_15k	4	89197070	2.9962	3	3	GKC	15000
Adam22	5	8073496	2.9754	3	3	GKC	15000
Kras	6	145186371	2.9522	3	3	GKC	15000
C230081A13Rik	9	56247931	2.2481	3	3	GKC	15000
Syne2	12	77151615	2.9948	3	3	GKC	15000
Gpc5	14	116597097	2.9978	3	3	GKC	15000
Grin3a	4	49722189	2.9943	2	3	GKC	15000
Arhgef16	4	153656219	2.6355	2	3	GKC	15000
CIS11:96783697_15k	11	96783697	2.7426	2	3	GKC	15000
Fam120a	13	49003589	2.0043	2	2	GKC	15000
Cul9	17	46656458	2.9904	2	3	GKC	15000
Ccnd3	17	47679200	1.9963	2	2	GKC	15000
Lrch2	X	144004796	1.9968	2	2	GKC	15000
CIS5:101806487_15k	5	101806487	2.7582	1	3	GKC	15000
1700061J05Rik	15	78206557	2.2961	3	3	GKC	30000
Vegfa	17	46184654	2.0856	3	3	GKC	30000
CIS7:119793053_75k	7	119793053	3.0777	4	4	GKC	75000
Ebf1	11	44449905	3.5976	4	5	GKC	75000
Gabpa	16	84861289	3.4943	5	5	GKC	120000
Smad6	9	63804405	4.3238	4	7	GKC	240000
Zc3h7b	15	81620516		4	4	MC	
AL669967.1|Usp9x	X	12696925		4	6	MC	
Gm12610	4	89197508		3	3	MC	
Adam22	5	8073960		3	3	MC	
Kras	6	145186264		3	3	MC	
C230081A13Rik	9	56243483		3	3	MC	
Syne2	12	77152252		3	3	MC	
Gpc5	14	116597107		3	3	MC	
Grin3a	4	49722761		2	3	MC	
Arhgef16	4	153655910		2	3	MC	
D030028A08Rik	11	96783929		2	3	MC	
Cul9|Gm16736	17	46655936		2	3	MC	
CIS5:101807040_MC	5	101807040		1	3	MC	

KCTSB10 pancreatic tumors were processed for transposon insertion, yielding a small number of CISs. CISs were scored by tumor frequency using the Gaussian kernel convolution framework (GKC) and Monte Carlo algorithms (MC), and listed here. Chr: chromosome, N: number of tumors from which the CIS was found, I, total number of insertions of the CIS in the indicated tumors

Supplementary Table 2 | Candidate CISs in pancreas tumors from KCTSB13 mice.

CISs were scored by tumor frequency using the Gaussian kernel convolution framework (GKC) and Monte Carlo algorithms (MC), Chr: chromosome; N: number of tumors from which the CIS was found; I, total number of insertions of the CIS in the indicated tumors**.**

Note: This Table has been uploaded as a separate excel file.

Supplementary Table 3a-b| List of non-redundant insertions.

A total of 88,084 non-redundant insertion sites from 198 tumors from KCTSB13 mice (Supplementary Table 3a (CRIUK_PPM_PANCREAS_20110408_SB13_INSERTIONS)) and 1,923 non-redundant insertion sites from 61 tumors from KCTSB10 mice (Supplementary Table 3b (CRIUK_PPM_PANCREAS_20110408_SB10_INSERTIONS)) were analysed.

The BED files of insertion sites conform to the first six columns of the standard BED format (http://genome.ucsc.edu/FAQ/FAQformat.html#format1). The fourth column contains detailed identifiers related to the processing of samples on the 454 Next Generation Sequencing machines. To determine specific samples from the fourth column, the first digit and period should be ignored. The following part of the identifier with the format XXX_YYY, uniquely defines the sample from which an insertion site originates.

Note: These Tables have been uploaded as a separate .ZIP.BED file.

Supplementary Table 4 | Comparison of KCTSB13 CISs to prior work in human PDA.

Human orthologues of the CISs listed in Supplementary Table 3 were evaluated for evidence of somatic mutations, using three data sets[5,29,30]. The columns amplification and homozygous deletion are marked if the gene occurred in the data published in[5]. For missense mutations, the designations S3, S4 and S7 correspond to the supplemental tables in[5] (S3 discovery screen, S4 prevalence screen and S7 gene with at least 2 mutations). The gene expression data denotes the relative expression alterations in either normal tissues (N) or tumor (T), if the mean of tag count between the 2 normal and the tumor samples was greater than 2.

Note: This Table has been uploaded as a separate excel file.

Supplementary Table 5 | PDA patient characteristics for the ICGC-APGI cohort

ICGC-APGI Cohort			
Variables	**N = 100 (%)**	**Median DSS (months)**	***P*-value(Logrank)**
Sex	**N = 100**		
Male	61 (61.0)	18.4	
Female	39 (39.0)	18.3	0.5467
Age (years)	**N = 100**		
Mean	66.9		
Median	68.0		
Range	34.0 – 90.0		
Outcome	**N = 100**		
Follow-up (months)	0.1 – 29.8		
Median follow-up	14.1		
Death due to pancreatic cancer	33 (33.0)		
Death other	9 (9.0)		
Death unknown	3 (3.0)		
Alive	55 (55.0)		
Lost to follow-up	0 (0.0)		
Stage[a]	**N = 100**		
I	8 (8.0)	17.4	
II	87 (87.0)	18.8	
III	1 (1.0)	----[b]	
IV	4 (4.0)	12.0	****[c]
T Stage[d]	**N = 100**		
T1	3 (3.0)		
T2	12 (12.0)	17.4	
T3	84 (84.0)		
T4	1 (1.0)	18.4	0.4297
N Stage	**N = 99**		
N0	24 (24.2)	17.4	
N1	75 (75.8)	18.4	0.4714
Grade[e]	**N = 100**		
I	4 (4.0)		
II	61 (61.0)	----	
III	33 (33.0)		
IV	2 (2.0)	15.1	0.0011
Tumor size	**N = 100**		
≤ 20mm	14 (14.0)	18.3	
> 20mm	86 (86.0)	18.4	0.8056
Margins	**N = 100**		
Clear	66 (66.0)	----	

Involved	34 (34.0)	13.9	0.0335
Tumor Location	**N = 100**		
Head	85 (85.0)	18.4	
Others	15 (15.0)	13.6	0.0488
Perineural Invasion	**N = 97**		
Negative	20 (20.6)	----	
Positive	77 (79.4)	17.4	0.0211
Vascular Invasion	**N = 96**		
Negative	39 (40.6)	----	
Positive	57 (59.4)	15.9	0.0348
Adj Chemotherapy	**N = 95**		
Yes	65 (68.4)	21.4	
No	30 (31.6)	12.0	0.0007
USP9X Expression	**N = 88**		
> 10^{th} Percentile	79 (89.8)	18.4	
≤ 10^{th} Percentile	9 (10.2)	8.7	0.0076

Clinical, histological and biochemical parameters were used to calculate P-values with Kaplan-Meier statistics Log-Rank test. [a] AJCC 7^{th} Edition; [b] Median survival has not been reached yet; [c] Rank test cannot be tested as one or more groups contained no censored observations; [d] Analysed as T1/2 Vs. T3/4; [e] Analysed as G1/2 Vs. G3/4. DSS: Disease Specific Survival.

Supplementary Table 6| Multivariate analyses for the ICGC-APGI cohort (clinico-pathological variables only)

Multivariate Analysis for ICGC-APGI Cohort			
	Variable	**Hazard Ratio (95% CI)**	***P*-Value**
A. (N= 100)	Grade (III & IV)	2.21 (1.00 – 4.88)	0.0510
	Margin Involvement (Positive)	0.92 (0.39 – 2.17)	0.8502
	Tumor Location (Body/Tail)	1.66 (0.62 – 4.46)	0.3098
	Perineural Invasion (Positive)	3.12 (0.86 – 11.2)	0.0831
	Vascular Invasion (Positive)	1.81 (0.69 – 4.74)	0.2236
	Adjuvant Chemotherapy	0.25 (0.11 – 0.56)	0.0014
B.	Grade (III & IV)	2.19 (0.99 – 4.83)	0.0521
	Tumor Location (Body/Tail)	1.65 (0.62 – 4.41)	0.3175
	Perineural Invasion (Positive)	3.05 (0.86 – 10.9)	0.0855
	Vascular Invasion (Positive)	1.76 (0.71 – 4.33)	0.2210
	Adjuvant Chemotherapy	0.26 (0.12 – 0.58)	0.0009
C.	Grade (III & IV)	2.34 (1.07 – 5.13)	0.0336
	Perineural Invasion (Positive)	3.50 (1.01 – 12.0)	0.0474
	Vascular Invasion (Positive)	1.57 (0.65 – 3.76)	0.3133
	Adjuvant Chemotherapy	0.26 (0.12 – 0.58)	0.0010
D. (Final Model)	Grade (III & IV)	2.60 (1.24 – 5.43)	0.0111
	Perineural Invasion (Positive)	4.33 (1.42 – 13.2)	0.0098
	Adjuvant Chemotherapy	0.26 (0.12 – 0.55)	0.0004

Cox regression analysis of clinical and pathological factors reveals that grade, perineural invasion and adjuvant therapy are prognostic factors for outcome.

Supplementary Table 7| Multivariate analyses for the ICGC-APGI cohort (clinico-pathological variables and USP9X)

Multivariate Analysis for ICGC-APGI Cohort			
	Variable	**Hazard Ratio (95% CI)**	***P*-Value**
A. Clinico-pathologic & USPS9X (N= 88)	Grade (III & IV)	1.68 (0.74 – 3.79)	0.2161
	Margin Involvement (Positive)	0.68 (0.28 – 1.68)	0.4080
	Tumor Location (Body/Tail)	1.43 (0.51 – 4.03)	0.4975
	Perineural Invasion (Positive)	3.04 (0.82 – 11.2)	0.0958
	Vascular Invasion (Positive)	2.33 (0.84 – 6.41)	0.1023
	Adjuvant Chemotherapy	0.20 (0.08 – 0.48)	0.0004
	USP9X mRNA Expression (High)	0.34 (0.11 – 1.06)	0.0619
B. Clinico-pathologic & USP9X	Grade (III & IV)	1.74 (0.78 – 3.89)	0.1772
	Margin Involvement (Positive)	0.71 (0.29 – 1.73)	0.4560
	Perineural Invasion (Positive)	3.38 (0.95 – 12.0)	0.0611
	Vascular Invasion (Positive)	2.07 (0.80 – 5.35)	0.1338
	Adjuvant Chemotherapy	0.20 (0.08 – 0.49)	0.0005
	USP9X mRNA Expression (High)	0.32 (0.10 – 0.98)	0.0460
C. Clinico-pathologic & USP9X	Grade (III & IV)	1.72 (0.77 – 3.85)	0.1872
	Perineural Invasion (Positive)	2.99 (0.86 – 10.4)	0.0845
	Vascular Invasion (Positive)	1.85 (0.74 – 4.61)	0.1884
	Adjuvant Chemotherapy	0.22 (0.10 – 0.52)	0.0005
	USP9X mRNA Expression (High)	0.36 (0.12 – 1.06)	0.0640
D. Clinico-pathologic & USP9X	Grade (III & IV)	1.86 (0.84 – 4.12)	0.1264
	Perineural Invasion (Positive)	4.07 (1.29 – 12.8)	0.0169
	Adjuvant Chemotherapy	0.22 (0.10 – 0.51)	0.0004
	USP9X mRNA Expression (High)	0.42 (0.14 – 1.22)	0.1093
E. Clinico-pathologic & USP9X (Final Model)	Perineural Invasion (Positive)	5.13 (1.64 – 16.1)	0.0049
	Adjuvant Chemotherapy	0.19 (0.08 – 0.44)	0.0001
	USP9X mRNA Expression (High)	0.32 (0.12 – 0.88)	0.0279

Stepwise cox regression analysis of USP9X in addition to clinical and pathological factors reveals that high USP9X expression is prognostic for a good outcome in PDA.

Supplementary Table 8 | USP9X and SMAD4 protein expression levels were assessed in autopsy samples from patients with metastatic pancreatic cancer.

Patient	Category	Burden	Mean USP9x	DPC4 Status	USP9x level
A52	Oligo	None	2	Intact	High
A53	Oligo	None	2	Intact	High
A65	Oligo	None	3	Intact	High
A77	Oligo	None	2	Lost	High
A106	Oligo	None	2	nd	High
A88	Oligo	1-10	2	Lost	High
A85	Oligo	1-10	2	nd	High
A73	Oligo	1-10	2	Intact	High
A7	Oligo	1-10	3	Intact	High
A33	Oligo	1-10	2	Intact	High
A96	Oligo	1-10	3	nd	High
A111	Oligo	1-10	2	Intact	High
A114	Oligo	1-10	3	nd	High
A40	Oligo	None	1	Intact	Low
A5	Oligo	None	1	Intact	Low
A15	Oligo	1-10	1	Lost	Low
A10	Widespread	11-100	2	Lost	High
A29	Widespread	11-100	2	Lost	High
A3	Widespread	11-100	2	Lost	High
A17	Widespread	>100	2	Lost	High
A28	Widespread	>100	3	nd	High
A55	Widespread	>100	2	Intact	High
A87	Widespread	>100	2	Intact	High
A89	Widespread	>100	3	Lost	High
A92	Widespread	>100	3	nd	High
A93	Widespread	>100	2	nd	High
A98	Widespread	>100	2.5	nd	High
A119	Widespread	>100	2	Lost	High
A31	Widespread	11-100	1	Intact	Low
A42	Widespread	11-100	1	Lost	Low
A80	Widespread	11-100	1	Lost	Low
A2	Widespread	>100	1	Lost	Low
A22	Widespread	>100	1	Lost	Low
A32	Widespread	>100	1	Lost	Low
A38	Widespread	>100	1	Lost	Low
A43	Widespread	>100	0.5	Intact	Low
A6	Widespread	>100	1	Lost	Low
A61	Widespread	>100	1	Lost	Low
A90	Widespread	>100	1	Intact	Low
A95	Widespread	>100	0.5	nd	Low
A117	Widespread	>100	1.5	Intact	Low
A120	Widespread	>100	1	nd	Low

Each patient was classified as having either oligometastatic (10 or fewer metastases) or widespread (>10) metastatic PDA. USP9X protein levels in PDA specimens were scored from 0-3; and a mean USP9X score was calculated by averaging the multiple measurements per patient. A mean score of 1.5 or lower was regarded as “low expression” for the purpose of the final classification of a given patient. The SMAD4 protein expression status for each patient was also evaluated. The USP9X levels did not correlate with SMAD4 expression (p=0.2151; Chi Squared test), consistent with the lack of association between USP9X and TGF beta. “nd”: not determined.

Supplementary Table 9a| Correlation of USP9X and ITCH expression in all patients with PDA

		USP9X (intensity 0-3)	ITCH (intensity 0-3)
Spearman-Rho Correlation coefficient	**USP9X (intensity 0-3)**	1	0.470
P-value (2-sided)			<0.01

USP9X protein expression closely associates with ITCH expression in PDA tumors. A total of 368 tumors from the entire cohort (n=404) were evaluated for the expression levels for both proteins.

Supplementary Table 9b | USP9X protein expression level distinguishes 4 groups in 376 surgically resected PDA tumors.

score	N	%
0 (absent)	51	13.6
1 (weak)	154	41
2 (medium)	137	36.4
3 (strong)	34	9

The USP9X immunohistochemistry score was used to separate all of the pancreatic tumors into four categories. A total of 376 tumors of the entire cohort (n=404), with evaluable staining for USP9x, were analysed. N: number of PDA/group.

Supplementary Table 9c | ITCH protein expression level distinguishes 4 groups in 375 surgically resected PDA tumors.

score	N	%
0 (absent)	115	30.5
1 (weak)	146	39
2 (medium)	112	30
3 (strong)	2	0.5

The ITCH immunohistochemistry score was used to separate all of the pancreatic tumors into four categories. A total of 375 tumors of the entire cohort (n=404), with evaluable staining for ITCH, were analysed. N: number of PDA/group.

Supplementary Table 10a | Clinical features of 317 PDA patients correlating with histopathological characteristics and USP9X and ITCH protein expression at the time of surgical resection.

		n	%	m. s. (days)	P-value
Total		317			
Sex					
	female	145	46	435	0.252
	male	172	54	551	
Age					
	Mean	64			
	Range	32-85			
Primary tumor					
	T 1/2	62	20	628	0.710
	T 3/4	255	80	491	
Grade					
	G 1/2	141	44	671	0.001*
	G 3/4	176	56	435	
	N0	106	33	600	0.065
	N1	211	67	476	
	R0	230	73	559	0.034*
	Rpos.	87	27	409	
	M0	247	78	554	0.006*#
	M1	24	8	511	
	Mx	46	14	419	
Adjuvant therapy					
	No	207	65	476	0.975
	Yes	110	35	555	
ITCH expression					
	No (0)	89	28	409	0.020*
	Yes (1-3)	228	72	540	
USP9X expression					
	No (0)	40	13	354	0.481
	Yes (1-3)	277	87	500	

Clinical, histological and biochemical parameters were used to calculate P-values with Kaplan-Meier statistics Log-Rank test. A star indicates the significant univariate factors for post operative survival time ($p < 0.05$); # denotes M0 vs. M1 tumors; m.s. = median survival.

Supplementary Table 10b| Cox regression model for the 317 patients with PDA (overall survival)

		P-value	Relative Risk	95% CI
Step 1	N (0 vs. positive)	0.606	0.918	0.665-1.269
	M (0 vs. positive)	0.197	0.714	0.428-1.192
	Adjuvant therapy (yes vs. no)	0.431	1.141	0.822-1.584
	Sex (female vs. male)	0.758	1.047	0.780-1.406
	Grade 1/2 vs. 3/4	0.030	0.706	0.515-0.967
	R (0 vs. positive)	0.649	0.919	0.638-1.323
	ITCH (absent vs. expressed)	0.133	1.339	0.915-1.958
	USP9X (absent vs. expressed)	0.687	0.897	0.529-1.521
	T (3/4 vs. 1/2)	0.515	1.131	0.781-1.636
Step 2	N (0 vs. positive)	0.614	0.920	0.666-1.271
	M (0 vs. positive)	0.208	0.721	0.434-1.199
	Adjuvant therapy (yes vs. no)	0.404	1.148	0.830-1.59
	Grade 1/2 vs. 3/4	0.027	0.703	0.514-0.961
	R (0 vs. positive)	0.626	0.914	0.636-1.313
	ITCH (absent vs. expressed)	0.126	1.345	0.920-1.964
	USP9X (absent vs. expressed)	0.694	0.900	0.531-1.525
	T (3/4 vs. 1/2)	0.511	1.132	0.782-1.637
Step 3	N (0 vs. positive)	0.607	0.919	0.665-1.269
	M (0 vs. positive)	0.192	0.714	0.431-1.185
	Adjuvant therapy (yes vs. no)	0.427	1.140	0.825-1.576
	Grade 1/2 vs. 3/4	0.024	0.698	0.511-0.954
	R (0 vs. positive)	0.592	0.906	0.632-1.3
	ITCH (absent vs. expressed)	0.131	1.299	0.925-1.822
	T (3/4 vs. 1/2)	0.488	1.139	0.788-1.646
Step 4	M (0 vs. positive)	0.181	0.708	0.427-1.174
	Adjuvant therapy (yes vs. no)	0.472	1.124	0.817-1.547
	Grade 1/2 vs. 3/4	0.018	0.690	0.507-0.939
	R (0 vs. positive)	0.597	0.907	0.632-1.301
	ITCH (absent vs. expressed)	0.127	1.302	0.928-1.827
	T (3/4 vs. 1/2)	0.516	1.129	0.783-1.629
Step 5	M (0 vs. positive)	0.117	0.680	0.419-1.102
	Adjuvant therapy (yes vs. no)	0.449	1.131	0.822-1.556
	Grade 1/2 vs. 3/4	0.013	0.680	0.502-0.921
	ITCH (absent vs. expressed)	0.145	1.282	0.918-1.789
	T (3/4 vs. 1/2)	0.581	1.106	0.773-1.582
Step 6	M (0 vs. positive)	0.132	0.693	0.429-1.117
	Adjuvant therapy (yes vs. no)	0.469	1.125	0.818-1.546
	Grade 1/2 vs. 3/4	0.013	0.680	0.502-0.922
	ITCH (absent vs. expressed)	0.147	1.280	0.917-1.786

Step 7	M (0 vs. positive)	0.112	0.680	0.423-1.094
	Grade 1/2 vs. 3/4	0.017	0.695	0.516-0.937
	ITCH (absent vs. expressed)	0.146	1.281	0.918-1.788
Step 8	M (0 vs. positive)	0.1	0.671	0.417-1.079
	Grade 1/2 vs. 3/4	0.016	0.693	0.515-0.933
Step 9	Grade 1/2 vs. 3/4	0.014	0.688	0.511-0.927

Cox Regression multivariate analysis with stepwise backward elimination based on the likelihood ratios reveals independent prognostic significance only for tumor grade.

Supplementary Table 11a | Clinical features of 176 high grade (grade 3-4) PDA patients, correlating with additional histopathological characteristics and USP9X and ITCH protein expression at the time of surgical resection.

		n	%	m.s. (days)	P-value
Total		176			
Sex					
	female	83	47	424	0.812
	male	93	53	470	
Age					
	Mean	64			
	Range	33-82			
Primary tumor					
	T 1/2	32	18	553	0.850
	T 3/4	144	82	435	
	N0	44	25	419	0.863
	N1	132	75	443	
	R0	127	70	435	0.811
	R1, R2	49	30	467	
	M0	144	92	478	0.676
	M1	12	8	498	
Adjuvant therapy					
	No	104	59	409	0.401
	Yes	72	41	532	
ITCH expression					
	No (0)	58	33	369	0.055
	Yes (1-3)	118	67	485	
USP9X expression					
	No (0)	23	13	329	0.037*
	Yes (1-3)	153	87	478	

Clinical, histological and biochemical parameters were used to calculate P-values with Kaplan-Meier statistics Log-Rank test. A star indicates that USP9X is the only significant univariate factor for post operative survival time ($p < 0.05$); m.s. = median survival.

Supplementary Table 11b | Cox regression model for high grade PDA patients (overall survival)

		P-value	Relative Risk	95% CI
Step 1	N (0 vs. pos.)	0.719	0.920	0.586-1.445
	M (0 vs. pos.)	0.989	0.995	0.463-2.138
	Adjuvant therapy (yes vs. no)	0.418	1.182	0.789-1.770
	Sex (female vs. male)	0.363	0.835	0.567-1.231
	R (0 vs. pos.)	0.963	1.011	0.627-1.631
	ITCH (absent vs. expressed)	0.328	1.275	0.784-2.073
	USP9X (absent vs. expressed)	0.199	1.554	0.793-3.048
	T (3/4 vs. 1/2)	0.969	0.990	0.605-1.620
Step 2	N (0 vs. pos.)	0.718	0.921	0.588-1.441
	Adjuvant therapy (yes vs. no)	0.414	1.182	0.791-1.767
	Sex (female vs. male)	0.357	0.835	0.569-1.226
	R (0 vs. pos.)	0.965	1.010	0.647-1.578
	ITCH (absent vs. expressed)	0.324	1.275	0.787-2.066
	USP9X (absent vs. expressed)	0.198	1.554	0.795-3.037
	T (3/4 vs. 1/2)	0.968	0.990	0.606-1.617
Step 3	N (0 vs. pos.)	0.714	0.920	0.589-1.437
	Adjuvant therapy (yes vs. no)	0.411	1.183	0.792-1.766
	Sex (female vs. male)	0.358	0.835	0.570-1.225
	R (0 vs. pos.)	0.971	1.008	0.653-1.555
	ITCH (absent vs. expressed)	0.324	1.275	0.787-2.065
	USP9X (absent vs. expressed)	0.192	1.556	0.800-3.027
Step 4	N (0 vs. pos.)	0.715	0.921	0.591-1.434
	Adjuvant therapy (yes vs. no)	0.407	1.181	0.797-1.750
	Sex (female vs. male)	0.355	0.835	0.570-1.224
	ITCH (absent vs. expressed)	0.318	1.276	0.791-2.060
	USP9X (absent vs. expressed)	0.186	1.559	0.808-3.010
Step 5	Adjuvant therapy (yes vs. no)	0.424	1.173	0.793-1.735
	Sex (female vs. male)	0.351	0.834	0.569-1.222
	ITCH (absent vs. expressed)	0.311	1.281	0.793-2.069
	USP9X (absent vs. expressed)	0.198	1.538	0.799-2.961
Step 6	Sex (female vs. male)	0.414	0.855	0.587-1.246
	ITCH (absent vs. expressed)	0.286	1.298	0.804-2.095
	USP9X (absent vs. expressed)	0.173	1.575	0.819-3.027
Step 7	ITCH (absent vs. expressed)	0.318	1.277	0.790-2.064
	USP9X (absent vs. expressed)	0.197	1.539	0.800-2.960
Step 8	USP9X (absent vs. expressed)	0.038	1.821	1.033-3.210

Cox Regression multivariate analysis with stepwise backward elimination based on the likelihood ratios reveals that USP9X absence is an independent poor prognostic factor for overall survival.

Supplemental Reference

39 Carlson, C. M., Frandsen, J. L., Kirchhof, N., McIvor, R. S. & Largaespada, D. A. Somatic integration of an oncogene-harboring Sleeping Beauty transposon models liver tumor development in the mouse. *Proc Natl Acad Sci U S A* **102**, 17059-17064 (2005).